PERGAMON Mathematical and Computer Modelling 35 (2002) 895–912

MATHEMATICAL AND COMPUTER MODELLING

www.elsevier.com/locate/mcm

A Mathematical Study of Peristaltic Transport of a Casson Fluid

A. V. MERNONE* AND J. N. MAZUMDAR
Department of Applied Mathematics
The University of Adelaide, Australia 5005
Anacleto.Mernone@dsto.defence.gov.au jmazunda@maths.adelaide.edu.au

S. K. LUCAS
School of Mathematics, University of South Australia
Mawson Lakes, Australia 5095
Stephen.Lucas@unisa.edu.au

(Received and accepted July 2000)

Abstract—In this paper, the peristaltic flow of rheologically complex physiological fluids when modelled by a non-Newtonian Casson fluid in a two-dimensional channel is considered. A perturbation series method of solution of the stream function for zeroth and first order in amplitude ratio is sought. Of interest is the difference between peristaltic transport of Newtonian and non-Newtonian fluids. It is found that Newtonian fluid is an important subclass of non-Newtonian fluids that may adequately represent some physiological phenomena. Analytical and numerical solutions are found for the zeroth and first order in stream function and compared to well-documented research in the literature. It is shown that for a Casson fluid, when certain approximations are made in the most generalized form of constitutive equation, the fluid may be adequately represented as an improvement of a Newtonian fluid.

Keywords—Mathematical modelling, Casson fluid, Peristalsis, Perturbation series method.

1. INTRODUCTION

As mentioned in an earlier paper in this sequel [1], peristalsis is the phenomenon in which a circumferential progressive wave of contraction or expansion (or both) propagates along a tube. If the tube is long enough, one might see several identical waves moving along the tube simultaneously. Peristalsis appears in many organisms and a variety of organs.

Peristalsis is now well known to physiologists to be one of the major mechanisms for fluid transport in many biological systems. In particular, peristaltic mechanisms may be involved in urine transport from the kidney to the bladder through the ureter, the movement of chyme in the gastrointestinal tract, the transport of spermatozoa in the ductus efferentes of the male

We would like to express sincere thanks to Drs. Peter Gill, Hilary Booth, and Paul McCann for their assistance during the preparation of this manuscript. Also, sincere gratitude goes to the reviewers for their valuable advice, most of which has been taken into consideration in the revised version of this paper.
*Author to whom all correspondence should be addressed.

0895-7177/02/$ - see front matter Typeset by $\mathcal{A}\mathcal{M}\mathcal{S}$-TEX
PII: S0895-7177(02)00058-4

reproductive tract and in the cervical canal, the movement of ova in the Fallopian tubes, the transport of lymph in the lymphatic vessels, and in the vascomotion in small blood vessels.

These flows also provide efficient means for sanitary fluid transport and are thus exploited in industrial peristaltic pumping and medical devices, for example, industrial applications of mechanical roller pumps using viscous fluids in the printing industry and the peristaltic transport of noxious fluid in the nuclear industry. In addition, peristaltic pumping occurs in many practical applications involving biomedical systems. Many modern medical devices have been designed on the principle of peristaltic pumping to transport fluids without internal moving parts, for example, the blood in the heart-lung machine.

The main motivation for any mathematical analysis of physiological fluid flows is to ultimately have a better understanding of the particular flow being modelled. If there is similarity between the results obtained from the analysis and experimental and clinical data, then the mechanism of flow can at least be explained. Because peristalsis is evident in many physiological flows, an accurate mathematical study can help explain the major contributing factors to many flows in the human body. When comparing results between the mathematical model and the experimental and clinical data, it is desirable that the data obtained from experimental research be as close as possible to the actual physiological parameter being analysed. That is to say, it may be necessary to take into account the effect the measuring instrument or device or procedure has on the data obtained.

The study of the mechanisms of peristalsis, in both mechanical and physiological situations, has become the subject of scientific research for quite some time. Since the first investigation of Latham [2], several theoretical and experimental attempts have been made to understand peristaltic action in different situations. Interest in peristaltic pumping has been quite recently stimulated by its relevance to ureteral function. As reliable and accurate urometric measurements became available through the work of Kiil [3] and Boyarski [4], several hydrodynamic models of ureteral function invoking peristalsis were attempted. The earliest models by Shapiro [5], Fung [6], and Shapiro *et al.* [7] were idealized and represented the peristalsis by an infinite train of sinusoidal waves in a two-dimensional channel; thus, they could pretend to only a qualitative relationship with the ureter. These models concerned themselves, in part, with offering an explanation of the biologically and medically important phenomenon of 'reflux'. One manifestation of this reflux is that bacteria sometimes travel from the bladder to the kidney against the mean urine flow. A similar phenomenon has been observed in the small bowel. These observations are puzzling because the travel times are too small to be explained by diffusion and also because retrograde peristaltic waves have not usually been observed. Later, Lykoudis [8] and Weinberg *et al.* [9] proposed models that represent ureteral waves more realistically. Fung [10] investigated the coupling between the forces of fluid-mechanical origin and the dynamics of the ureteral muscle. Some of these models showed that observed urometric pressure pulses and flow rates could be accounted for by assuming internal dimensions of the ureter which seem physiologically plausible. But ureteral physiology has not been the only motivation for the study of peristalsis.

Burns and Parkes [11] and Hanin [12] contributed to the theory of peristaltic pumping without reference to physiological applications. Barton and Raynor [13] made a calculation based on peristalsis theory of the time required for chyme to traverse the small intestine and found that this calculation compared favorably with observed values. In addition, Fung [10] studied peristaltic flow taking muscle action in the tube wall into account. Some new examples of peristalsis were given in [14]. Considerable experimental investigations of peristaltic pumping have also been undertaken, for example, in [2,9,15–20]. Most of the theoretical investigations have been carried out by assuming blood and other physiological fluids behave like a Newtonian fluid. Although this approach may provide a satisfactory understanding of the peristaltic mechanism in the ureter, it fails to provide a satisfactory model when the peristaltic mechanism is involved in small blood vessels, lymphatic vessels, intestine, ductus efferentes of the male reproductive transport, and in the transport of spermatozoa in the cervical canal. It has now been accepted that most of

the physiological fluids behave like non-Newtonian fluids. But, it appears that no quantitative rigorous attempt has been made to understand the problem of a non-Newtonian fluid before the investigation of Raju and Devanathan [21] in the case of small wave amplitude. Subsequently, Srivastava and Srivastava [22] investigated the problem of peristaltic transport of blood assuming a single-layered Casson fluid and ignoring the presence of a peripheral layer. Later on, Srivastava [23] considered the axisymmetric flow of a Casson fluid in a circular nonuniform tube. More recently, Siddiqui *et al.* [24] investigated peristaltic motion of a non-Newtonian fluid modelled with a constitutive equation for a second-order fluid for the case of a planar channel. A perturbation series was used representing parameters such as curvature, inertia, and the non-Newtonian character of the fluid. Tang and Rankin [25] proposed a mathematical model for peristaltic motion of a nonlinear viscous flow where they used an iterative method to solve a free boundary problem. Das and Batra [26] studied the fully developed, steady flow of a Casson fluid through a curved tube for small values of Dean number. A plug core formation region at the centre is considered where the shear stress is not sufficient to exceed the yield value. Elshehawey *et al.* [27] consider the problem of peristaltic transport of a non-Newtonian (Carreau) fluid in a nonuniform channel under zero Reynolds number with long wavelength approximation. The problem is formulated using a perturbation expansion in terms of a variant of Weissenberg number. They find that pressure rise and friction force are smaller than the corresponding values in the case of uniform geometry. However, in the present paper, we propose to study peristaltic transport of physiological fluids in a planar channel using the most generalized form of constitutive equation, for Casson fluid, as given by Fung [28]. The final analysis is done by using a perturbation method in the same way as was done in our previous paper [1]. To the author's knowledge, the use of this generalized equation has not been considered previously in the literature.

2. PROBLEM FORMULATION

2.1. Dimensionless Variables in a Two-Dimensional Channel

$$x' = \frac{x}{d}, \quad y' = \frac{y}{d}, \quad u' = \frac{u}{c}, \quad v' = \frac{v}{c}, \quad \psi' = \frac{\psi}{cd},$$

$$\tilde{\alpha} = \frac{2\pi d}{\lambda}, \quad \varepsilon = \frac{A}{d}, \quad t' = \frac{ct}{d}, \quad G' = \frac{G}{d}, \quad p' = \frac{p}{\rho c^2}.$$

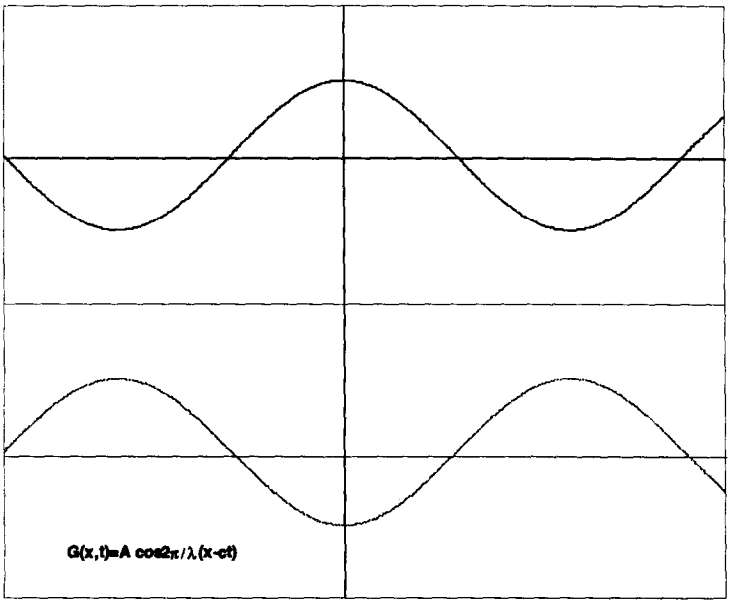

Figure 1. Peristaltic flow in a two-dimensional channel.

2.2. Statement of Problem

Consider the peristaltic motion of a non-Newtonian fluid, modelled as a Casson fluid in a two-dimensional channel, where d is the undeformed width of the channel and the channel is considered to be infinitely long; A represents the amplitude of the sinusoidal waves travelling along the channel at velocity c; λ is the wavelength (Figure 1). A rectangular coordinate system is chosen for the channel with x along the centre line and y normal to it. Let u and v be the longitudinal and transverse velocity components, respectively. It is assumed that an infinite train of sinusoidal waves progresses along the walls in the x direction. The vertical displacements for the upper and lower walls are G and $-G$ for peristaltic flow at time t, where G is defined by

$$G(x,t) = A\cos\frac{2\pi}{\lambda}(x-ct). \tag{1}$$

We assume that there is no motion of the wall in the longitudinal direction (extensible or elastic wall).

For the case of peristaltic pumping of a Casson fluid in a planar channel, the stress-strain relationship in tensor format is given by Fung [28] as

$$\sigma_{ij} = -p\delta_{ij} + 2\mu(J_2)V_{ij}, \tag{2}$$

where

$$\begin{aligned}\mu(J_2) &= \left[\left(\eta^2 J_2\right)^{1/4} + 2^{-1/2}\tau_y^{1/2}\right]^2 J_2^{-1/2} = \left[\eta^{1/2} + 2^{-1/2}\tau_y^{1/2}J_2^{-1/4}\right]^2 \\ &= \left[\alpha + \beta J_2^{-1/4}\right]^2 = \mu \qquad \text{(say)}.\end{aligned} \tag{3}$$

Here, we have denoted

$$\alpha = \eta^{1/2} : \beta = 2^{-1/2}\tau_y^{1/2}, \tag{4}$$

where η is the Casson coefficient of viscosity, and τ_y is the yield stress. Here,

$$V_{ij} = \frac{1}{2}\left(\frac{\partial u_i}{\partial x_j} + \frac{\partial u_j}{\partial x_i}\right) \tag{5}$$

and

$$J_2 = \frac{1}{2}V_{ij}V_{ij} = \frac{1}{2}\left(V_{11}^2 + V_{22}^2 + 2V_{12}^2\right), \tag{6}$$

where

$$V_{11} = \frac{\partial u}{\partial x}, \qquad V_{22} = \frac{\partial v}{\partial y}, \qquad V_{12} = V_{21} = \frac{1}{2}\left(\frac{\partial u}{\partial y} + \frac{\partial v}{\partial x}\right).$$

2.3. Mathematical Modelling of a Casson Fluid in a Two-Dimensional Channel

Substituting equations (2)–(6) into the basic equations for continuity and momentum, respectively, given by

$$\operatorname{div}\underline{q} = 0 \tag{7}$$

and

$$\rho\frac{Dq_i}{Dt} = \frac{\partial}{\partial x_j}\sigma_{ij}, \tag{8}$$

we have

$$\rho\left(\frac{\partial u}{\partial t} + u\frac{\partial u}{\partial x} + v\frac{\partial u}{\partial y}\right) = -\frac{\partial p}{\partial x} + 2\mu_x\frac{\partial u}{\partial x} + \mu_y\left(\frac{\partial u}{\partial y} + \frac{\partial v}{\partial x}\right) + 2\mu\frac{\partial^2 u}{\partial x^2} + \mu\frac{\partial}{\partial y}\left(\frac{\partial u}{\partial y} + \frac{\partial v}{\partial x}\right),$$

which, using continuity, reduces to

$$\rho\left(\frac{\partial u}{\partial t} + u\frac{\partial u}{\partial x} + v\frac{\partial u}{\partial y}\right) = -\frac{\partial p}{\partial x} + 2\mu_x\frac{\partial u}{\partial x} + \mu_y\left(\frac{\partial u}{\partial y} + \frac{\partial v}{\partial x}\right) + \mu\nabla^2 u. \tag{9}$$

Similarly,

$$\rho\left(\frac{\partial v}{\partial t}+u\frac{\partial v}{\partial x}+v\frac{\partial v}{\partial y}\right)=-\frac{\partial p}{\partial y}+2\mu_y\frac{\partial v}{\partial y}+\mu_x\left(\frac{\partial u}{\partial y}+\frac{\partial v}{\partial x}\right)+\mu\nabla^2 v. \tag{10}$$

Defining a stream function as $u=\psi_y$ and $v=-\psi_x$ we obtain from equations (9) and (10), respectively,

$$\rho(\psi_{yt}+\psi_y\psi_{xy}-\psi_x\psi_{yy})=-\frac{\partial p}{\partial x}+2\mu_x\psi_{xy}+\mu_y(\psi_{yy}-\psi_{xx})+\mu\nabla^2\psi_y \tag{11}$$

and

$$\rho(-\psi_{xt}-\psi_y\psi_{xx}+\psi_x\psi_{xy})=-\frac{\partial p}{\partial y}-2\mu_y\psi_{xy}+\mu_x(\psi_{yy}-\psi_{xx})-\mu\nabla^2\psi_x, \tag{12}$$

where

$$\mu_x=\frac{\partial}{\partial x}[\mu(J_2)], \qquad \text{and} \qquad \mu_y=\frac{\partial}{\partial y}[\mu(J_2)].$$

2.4. Solution Procedure (Zeroth-Order Approximation)

Expressing stream function ψ, pressure p, and μ as a series in terms of amplitude ratio $\varepsilon=A/d$, where A is the amplitude and d is the undeformed width of the channel (Figure 1), we have

$$\psi=\psi_0+\varepsilon\psi_1+\varepsilon^2\psi_2+O\left(\varepsilon^3\right), \tag{13}$$

$$p=p_0+\varepsilon p_1+\varepsilon^2 p_2+O\left(\varepsilon^3\right), \tag{14}$$

$$\mu=\mu_0+\varepsilon\mu_1+\varepsilon^2\mu_2+O\left(\varepsilon^3\right), \tag{15}$$

where it is assumed that ψ_0 is a function of y only, i.e., $\psi_0=\psi_0(y)$, because of zeroth-order axial pressure gradient. We finally obtain from equations (11) and (13)–(15) after collecting coefficients of ε^0,

$$\frac{\partial p_0}{\partial x}=2\mu_{0x}\psi_{0yx}+\mu_{0y}\psi_{0yy}-\mu_{0y}\psi_{0xx}+\mu_0\psi_{0xxy}+\mu_0\psi_{0yyy},$$

that is,

$$\frac{\partial p_0}{\partial x}=\mu_{0y}\psi_{0yy}+\mu_0\psi_{0yyy}. \tag{16}$$

Therefore,

$$\frac{\partial p_0}{\partial x}=\frac{\partial}{\partial y}(\mu_0\psi_{0yy}). \tag{17}$$

We now need to find the zeroth-order expression for $\mu_0=\mu(J_2)_0$. From equation (6) and expanding and substituting, we have

$$\begin{aligned} J_2&=\frac{1}{2}\left\{\left(\frac{\partial u}{\partial x}\right)^2+\left(\frac{\partial v}{\partial y}\right)^2+\frac{2}{4}\left(\frac{\partial u}{\partial y}+\frac{\partial v}{\partial x}\right)^2\right\}=\frac{1}{2}\left\{\psi_{xy}^2+\psi_{xy}^2+\frac{1}{2}(\psi_{yy}-\psi_{xx})^2\right\}\\ &=\left\{\psi_{xy}^2+\frac{1}{4}(\psi_{yy}-\psi_{xx})^2\right\}. \end{aligned} \tag{18}$$

Therefore we have, after introducing equations (13), (15), and (18),

$$\mu(J_2)=\left\{\alpha+\beta\left[\frac{1}{4}\left(\psi_{0yy}^2+2\varepsilon\psi_{0yy}(\psi_{1yy}-\psi_{1xx})\right)\right]^{-1/4}+O\left(\varepsilon^2\right)\right\}^2. \tag{19}$$

Neglecting $O(\varepsilon^2)$ and higher in equation (19) and expanding, we have

$$\mu(J_2)\approx\left\{\alpha+\beta\left(\frac{1}{4}\right)^{-1/4}\psi_{0yy}^{-1/2}\left(1-\frac{\varepsilon}{2}\psi_{0yy}^{-1}(\psi_{1yy}-\psi_{1xx})\right)\right\}^2, \tag{20}$$

which after further expansion and collecting terms in amplitude ratio for the first two terms and using equation (15) yield equations for $\mu_0 = \mu(J_2)_0$ and $\mu_1 = \mu(J_2)_1$ as

$$\mu_0 = \alpha^2 + 2\sqrt{2}\alpha\beta\psi_{0yy}^{-1/2} + 2\beta^2\psi_{0yy}^{-1}, \tag{21}$$

$$\mu_1 = -\alpha\beta\sqrt{2}\psi_{0yy}^{-3/2}(\psi_{1yy} - \psi_{1xx}) - 2\beta^2\psi_{0yy}^{-2}(\psi_{1yy} - \psi_{1xx}). \tag{22}$$

Solving equation (17) by using equation (21) and nondimensionalising and applying the symmetry boundary condition $\psi_{0yy}(0) = 0$, we have

$$Ky + L = \mu_0\psi_{0yy},$$

where

$$K = \rho\sqrt{c^3 d}\,\frac{\partial p_0}{\partial x} \qquad \text{and} \qquad L = 2\beta^2. \tag{23}$$

Our equation to solve for $\psi_0(y)$ then becomes

$$\alpha^2\psi_{0yy} + 2\sqrt{2}\alpha\beta\psi_{0yy}^{1/2} - Ky = 0. \tag{24}$$

If we set

$$\psi_{0yy} = W^2, \tag{25}$$

then equation (24) becomes a quadratic in W as

$$\alpha^2 W^2 + 2\sqrt{2}\alpha\beta W - Ky = 0, \tag{26}$$

whose roots are given by

$$W = -\sqrt{2}\frac{\beta}{\alpha} \pm \frac{1}{\alpha}\sqrt{2\beta^2 + Ky}. \tag{27}$$

Using equations (25) and (27), we obtain

$$\psi_{0yy} = \left(-\sqrt{2}\frac{\beta}{\alpha} \pm \frac{1}{\alpha}\sqrt{2\beta^2 + Ky}\right)^2. \tag{28}$$

But, the symmetry boundary condition $\psi_{0yy}(0) = 0$ demands only the positive sign to be valid; therefore,

$$\psi_{0yy} = \left(-\sqrt{2}\frac{\beta}{\alpha} + \frac{1}{\alpha}\sqrt{2\beta^2 + Ky}\right)^2. \tag{29}$$

Integrating equation (29) twice we obtain

$$\psi_0(y) = \frac{2\beta^2}{\alpha^2}y^2 + \frac{K}{6\alpha^2}y^3 - \frac{8\sqrt{2}\beta}{15K^2\alpha^2}\left(2\beta^2 + Ky\right)^{5/2} + Ay + B, \tag{30}$$

where A and B are constants of integration.

Using the boundary conditions $\psi_{0y}(1) = 0$ and $\psi(0) = 0$, we find

$$A = \frac{4\sqrt{2}\beta}{3\alpha^2 K}\left(2\beta^2 + K\right)^{3/2} - \frac{4\beta^2}{\alpha^2} - \frac{K}{2\alpha^2}, \tag{31}$$

$$B = \frac{8\sqrt{2}\beta}{15K^2\alpha^2}\left(2\beta^2\right)^{5/2}. \tag{32}$$

If we let $\beta \to 0$, that is, $\tau_y \to 0$ from equation (4), we obtain the Newtonian case in the form

$$\psi_0(y) = -\frac{K}{2\alpha^2}\left(y - \frac{y^3}{3}\right),$$

which coincides with the literature [6].

We now seek to determine the dimensionless pressure rise, Δp_0, where

$$\Delta p_0 = \int_0^1 \frac{\partial p_0}{\partial x}\, dx. \tag{33}$$

The flow rate, q, is given by

$$q = \int_0^1 u\, dy = \int_0^1 \frac{\partial \psi}{\partial y}\, dy = \psi(1) - \psi(0); \tag{34}$$

therefore, from equations (30)–(32),

$$\psi(1) - \psi(0) = -\frac{2\beta^2}{\alpha^2} - \frac{K}{3\alpha^2} + \frac{4\sqrt{2}}{3\alpha^2 K}\left(2\beta^2 + K\right)^{3/2} = q. \tag{35}$$

Applying expansion gives

$$q = \frac{2\beta^2}{\alpha^2} - \frac{K}{3\alpha^2} + \frac{16\beta^4}{3\alpha^2 K}. \tag{36}$$

Separating the pressure gradient after solving for quadratic in K, and using equation (23), gives

$$\frac{\partial p_0}{\partial x} = \frac{K}{\rho\sqrt{c^3 d}} = \frac{1}{\rho\sqrt{c^3 d}}\left\{-\frac{1}{2}\left(3\alpha^2 q - 6\beta^2\right) \pm \frac{1}{2}\sqrt{9\alpha^4 q^2 + 100\beta^4 - 36\alpha^2 q\beta^2}\right\}. \tag{37}$$

Hence, using equation (33), pressure rise is

$$\begin{aligned}
\Delta p_0 &= \frac{1}{\rho\sqrt{c^3 d}} \int_0^1 \left\{-\frac{1}{2}\left(3\alpha^2 q - 6\beta^2\right) \pm \frac{1}{2}\sqrt{9\alpha^4 q^2 + 100\beta^4 - 36\alpha^2 q\beta^2}\right\} dx, \\
&\text{because } -\frac{1}{2}\left(3\alpha^2 q - 6\beta^2\right) \pm \frac{1}{2}\sqrt{9\alpha^4 q^2 + 100\beta^4 - 36\alpha^2 q\beta^2} = \text{constant}, \\
\Delta p_0 &= \frac{1}{\rho\sqrt{c^3 d}}\left\{-\frac{1}{2}\left(3\alpha^2 q - 6\beta^2\right) \pm \frac{1}{2}\sqrt{9\alpha^4 q^2 + 100\beta^4 - 36\alpha^2 q\beta^2}\right\}.
\end{aligned} \tag{38}$$

However, the condition $\beta = 0$ implies that only the negative sign of the quadratic is valid; therefore,

$$\Delta p_0 = \frac{1}{\rho\sqrt{c^3 d}}\left\{-\frac{1}{2}\left(3\alpha^2 q - 6\beta^2\right) - \frac{1}{2}\sqrt{9\alpha^4 q^2 + 100\beta^4 - 36\alpha^2 q\beta^2}\right\}. \tag{39}$$

This is graphically depicted in Figure 2.

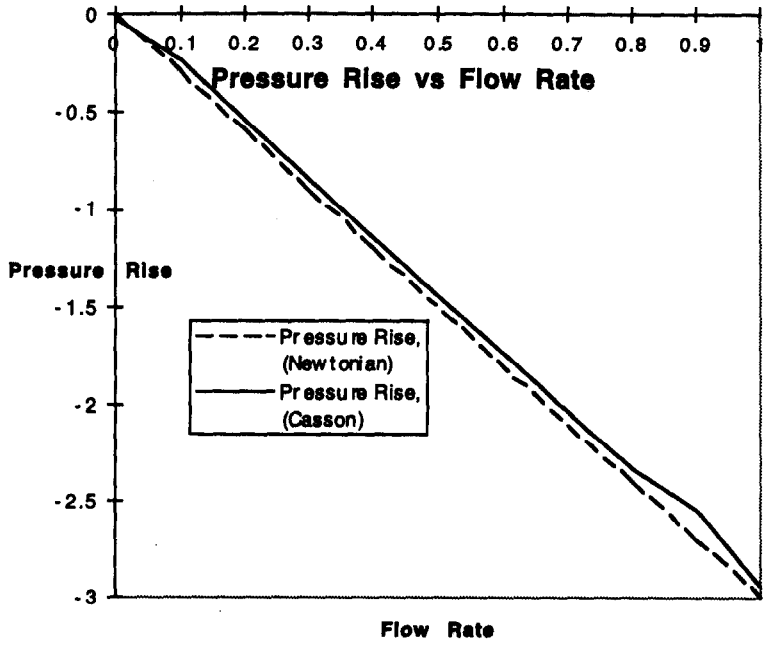

Figure 2. Pressure rise vs. flow rate.

2.5. Solution Procedure (First-Order Approximation)

We now look at the procedure for determining $\psi_1(x,y,t)$. The boundary conditions for $\psi_1(x,y,t)$ are derived as follows. Assuming that there is no horizontal displacement of the tube walls during the peristaltic motion, the boundary conditions at the walls are

$$\text{no-slip condition:} \quad u = 0, \qquad \text{at } y = \pm[d + G(x,t)], \tag{40a}$$

$$\text{impermeable condition:} \quad v = \pm\frac{\partial}{\partial t}G(x,t), \quad \text{at } y = \pm[d + G(x,t)]. \tag{40b}$$

Using $G(x,t) = A\cos(2\pi/\lambda)(x-ct)$ and equation (13) and nondimensionalising as defined above, we obtain

$$\psi_y = 0, \qquad \text{at } y = \pm[1 + \varepsilon\cos\tilde{\alpha}(x-t)], \tag{41a}$$

$$\psi_x = \mp\frac{2\pi Ac}{\lambda}\sin\frac{2\pi}{\lambda}(x-ct) = \mp\tilde{\alpha}\varepsilon\sin\tilde{\alpha}(x-t), \qquad \text{at } y = \pm[1 + \varepsilon\cos\tilde{\alpha}(x-t)]. \tag{41b}$$

The boundary conditions (41) can be written using Taylor series expansions about $y = \pm(1+G)$ where here $G = \varepsilon\cos\tilde{\alpha}(x-t)$ as, after equating terms of the same order in ε, on either side of the equations, which gives

$$\psi_y(\pm1) \pm G\psi_{yy}(\pm1) + \frac{G^2}{2}\psi_{yyy}(\pm1) \pm O\left(G^3\right) = 0, \tag{42a}$$

$$\psi_x(\pm1) \pm G\psi_{xy}(\pm1) + \frac{G^2}{2}\psi_{xyy}(\pm1) \pm O\left(G^3\right) = \mp\tilde{\alpha}\varepsilon\sin\tilde{\alpha}(x-t). \tag{42b}$$

Substituting equation (13) into equation (42) and collecting terms of the same order in ε gives

$$\begin{aligned} &\psi_{0y}(\pm1) = 0, \qquad \psi_{1y}(\pm1) \pm \psi_{0yy}(\pm1)\cos\tilde{\alpha}(x-t) = 0, \\ &\psi_{0x}(\pm1) = 0, \qquad \psi_{1x}(\pm1) \pm \psi_{0xy}(\pm1)\cos\tilde{\alpha}(x-t) = \mp\tilde{\alpha}\sin\tilde{\alpha}(x-t), \end{aligned} \tag{43}$$

and so on for higher order terms in ε. Taking the positive sign of the boundary conditions as given in equation (43) yields the boundary conditions as

$$\psi_{1y}(1) = -\psi_{0yy}(1)\cos\tilde{\alpha}(x-t), \tag{44a}$$

$$\psi_{1x}(1) = -\tilde{\alpha}\sin\tilde{\alpha}(x-t). \tag{44b}$$

From these boundary conditions, it can be assumed that $\psi_1(x,y,t)$ can be obtained in the form

$$\psi_1(x,y,t) = f(y)\cos\tilde{\alpha}(x-t) + g(y)\sin\tilde{\alpha}(x-t). \tag{45}$$

Eliminating the pressure terms in equations (11) and (12) by cross-differentiation and subtraction, the following equation is obtained:

$$\begin{aligned} \rho\left(\nabla^2\psi_t + \psi_y\nabla^2\psi_x - \psi_x\nabla^2\psi_y\right) &= 4\mu_{xy}\psi_{yx} + 2\mu_x\psi_{yyx} + \mu_{yy}(\psi_{yy} - \psi_{xx}) + \mu_y(\psi_{yyy} - \psi_{xxy}) \\ &\quad + \mu_y\nabla^2\psi_y + \mu\nabla^2\psi_{yy} + 2\mu_y\psi_{xxy} - \mu_{xx}(\psi_{yy} - \psi_{xx}) \\ &\quad - \mu_x(\psi_{yyx} - \psi_{xxx}) + \mu_x\nabla^2\psi_x + \mu\nabla^2\psi_{xx}. \end{aligned} \tag{46}$$

By substituting equation (45) for $\psi_1(x,y,t)$ and equation (29) for $\psi_0(y)$ into equation (46), and collecting coefficients of $\cos\tilde{\alpha}(x-t)$ and $\sin\tilde{\alpha}(x-t)$ on either side of the resulting equation, two differential equations for $f(y)$ and $g(y)$ are obtained.

Due to the length and complexity of these equations, approximate solutions are obtained by assuming that the parameter $\tilde{\alpha}$, which is $(2\pi d)/\lambda$, is small. As a first approximation, the terms

of order $\tilde{\alpha}^2$ and higher can be neglected; as a second approximation, the terms of order $\tilde{\alpha}^3$ and higher can be neglected, and so on.

Hence, the following equation is obtained from equation (45) by expanding in a perturbations series as indicated in equations (13)–(15) after collecting terms of the first order in amplitude ratio, ε:

$$\begin{aligned}\rho\sqrt{c^3 d}(\psi_{1yyt} + \psi_{0y}\psi_{1yyx} - \psi_{1x}\psi_{0yyy}) = \mu_{0yy}\psi_{1yy} + \mu_{1yy}\psi_{0yy} + 2\mu_{0y}\psi_{1yyy} \\ +2\mu_{1y}\psi_{0yyy} + \mu_0\psi_{1yyyy} + \mu_1\psi_{0yyyy},\end{aligned} \tag{47}$$

where $\mu_0, \mu_{0y}, \mu_{0yy}$ and $\mu_1, \mu_{1y}, \mu_{1yy}$ are extensive and complicated equations and are obtained from equation (21) and (22), respectively, as follows:

$$\mu_{0y} = -\sqrt{2}\alpha\beta\psi_{0yy}^{-3/2}\psi_{0yyy} - \beta^2\psi_{0yy}^{-2}\psi_{0yyy}, \tag{48}$$

$$\mu_{0yy} = \frac{3\alpha\beta}{\sqrt{2}}\psi_{0yy}^{-5/2}\psi_{0yyy}^2 - \sqrt{2}\alpha\beta\psi_{0yy}^{-3/2}\psi_{0yyyy} + 4\beta^2\psi_{0yy}^{-3}\psi_{0yyy}^2 - 2\beta^2\psi_{0yy}^{-2}\psi_{0yyyy}, \tag{49}$$

$$\mu_{1y} = \frac{3\alpha\beta}{\sqrt{2}}\psi_{0yy}^{-5/2}\psi_{0yyy}\psi_{1yy} - \sqrt{2}\alpha\beta\psi_{0yy}^{-3/2}\psi_{1yyy} + 4\beta^2\psi_{0yy}^{-3}\psi_{0yyy}\psi_{1yy} - 2\beta^2\psi_{0yy}^{-2}\psi_{1yyy}, \tag{50}$$

$$\begin{aligned}\mu_{1y} = &-\frac{15\alpha\beta}{2\sqrt{2}}\psi_{0yy}^{-7/2}\psi_{0yyy}^2\psi_{1yy} + \frac{3\alpha\beta}{\sqrt{2}}\psi_{0yy}^{-5/2}\psi_{0yyyy}\psi_{1yy} + \frac{6\alpha\beta}{\sqrt{2}}\psi_{0yy}^{-5/2}\psi_{0yyy}\psi_{1yyy} \\ &- \sqrt{2}\alpha\beta\psi_{0yy}^{-3/2}\psi_{1yyyy} - 12\beta^2\psi_{0yy}^{-4}\psi_{0yyy}^2\psi_{1yy} + 4\beta^2\psi_{0yy}^{-3}\psi_{0yyyy}\psi_{1yy} \\ &+ 8\beta^2\psi_{0yy}^{-3}\psi_{0yyy}\psi_{1yyy} - 2\beta^2\psi_{0yy}^{-2}\psi_{1yyy}.\end{aligned} \tag{51}$$

After substituting for the various terms in equation (47) and collecting terms and remembering the approximation made on terms in the parameter $\tilde{\alpha}$, the following ordinary differential equation is:

$$\begin{aligned}&\rho\sqrt{c^3 d}\left\{\begin{array}{c}\tilde{\alpha}f''\sin\tilde{\alpha}(x-t) - \tilde{\alpha}g''\cos\tilde{\alpha}(x-t) + \left[\dfrac{4\beta^2}{\alpha^2}y + \dfrac{k}{2\alpha^2}y^2 - \dfrac{4\beta\sqrt{2}}{3k\alpha^2}\left(2\beta^2+ky\right)^{3/2} + A\right] \\ \times\left(-\tilde{\alpha}f''\sin\tilde{\alpha}(x-t) + \tilde{\alpha}g''\cos\tilde{\alpha}(x-t)\right) \\ -\left(-\tilde{\alpha}f\sin\tilde{\alpha}(x-t) + \tilde{\alpha}g\cos\tilde{\alpha}(x-t)\right)\dfrac{k^2}{4\beta^2\alpha^2}y\end{array}\right\} \\ &= \left(\frac{k^2y}{4\beta^2\alpha^2}\right)^2\left(f''\cos\tilde{\alpha}(x-t) + g''\sin\tilde{\alpha}(x-t)\right)\frac{3\alpha\beta}{2\sqrt{2}}\left[\frac{4\beta^2}{\alpha^2} + \frac{k}{\alpha^2}y - \frac{2\beta\sqrt{2}}{\alpha^2}\left(2\beta^2+ky\right)^{1/2}\right]^{-5/2} \\ &\quad - \left(\frac{ky}{4\beta^2\alpha^2}\right)\left(f'''\cos\tilde{\alpha}(x-t) + g'''\sin\tilde{\alpha}(x-t)\right) \\ &\quad \times\alpha\beta\sqrt{2}\left[\frac{4\beta^2}{\alpha^2} + \frac{k}{\alpha^2}y - \frac{2\beta\sqrt{2}}{\alpha^2}\left(2\beta^2+ky\right)^{1/2}\right]^{-3/2} \\ &\quad + \alpha^2\left(f^{iv}\cos\tilde{\alpha}(x-t) + g^{iv}\sin\tilde{\alpha}(x-t)\right) - \left(\frac{k^2}{4\alpha^2\beta^2} - \frac{3k^3}{16\beta^4\alpha^2}y\right)\frac{\alpha\beta}{\sqrt{2}} \\ &\quad \times\left(f''\cos\tilde{\alpha}(x-t) + g''\sin\tilde{\alpha}(x-t)\right)\left[\frac{4\beta^2}{\alpha^2} + \frac{k}{\alpha^2}y - \frac{2\beta\sqrt{2}}{\alpha^2}\left(2\beta^2+ky\right)^{1/2}\right]^{-3/2} \\ &\quad + \alpha\beta\sqrt{2}\left[\frac{4\beta^2}{\alpha^2} + \frac{k}{\alpha^2}y - \frac{2\beta\sqrt{2}}{\alpha^2}\left(2\beta^2+ky\right)^{1/2}\right]^{-1/2}\left(f^{iv}\cos\tilde{\alpha}(x-t) + g^{iv}\sin\tilde{\alpha}(x-t)\right),\end{aligned} \tag{52}$$

where the constant A is given in equation (31).

Collecting coefficients of $\cos\tilde{\alpha}(x-t)$ in equation (52) gives

$$\begin{aligned}
&\rho\sqrt{c^3 d}\left\{-\tilde{\alpha}g'' + \left[\frac{4\beta^2}{\alpha^2}y + \frac{k}{2\alpha^2}y^2 - \frac{4\beta\sqrt{2}}{3k\alpha^2}\left(2\beta^2+ky\right)^{3/2} + A\right](\tilde{\alpha}g'') - (\tilde{\alpha}g)\frac{k^2}{4\beta^2\alpha^2}y\right\} \\
&\quad = \left(\frac{k^2 y}{4\beta^2\alpha^2}\right)^2 (f'')\frac{3\alpha\beta}{2\sqrt{2}}\left[\frac{4\beta^2}{\alpha^2} + \frac{k}{\alpha^2}y - \frac{2\beta\sqrt{2}}{\alpha^2}\left(2\beta^2+ky\right)^{1/2}\right]^{-5/2} \\
&\quad - \left(\frac{ky}{4\beta^2\alpha^2}\right)(f''')\alpha\beta\sqrt{2}\left[\frac{4\beta^2}{\alpha^2} + \frac{k}{\alpha^2}y - \frac{2\beta\sqrt{2}}{\alpha^2}\left(2\beta^2+ky\right)^{1/2}\right]^{-3/2} \\
&+\alpha^2(f^{iv}) - \left(\frac{k^2}{4\alpha^2\beta^2} - \frac{3k^3}{16\beta^4\alpha^2}y\right)\frac{\alpha\beta}{\sqrt{2}}(f'')\left[\frac{4\beta^2}{\alpha^2} + \frac{k}{\alpha^2}y - \frac{2\beta\sqrt{2}}{\alpha^2}\left(2\beta^2+ky\right)^{1/2}\right]^{-3/2} \\
&\quad + \alpha\beta\sqrt{2}\left[\frac{4\beta^2}{\alpha^2} + \frac{k}{\alpha^2}y - \frac{2\beta\sqrt{2}}{\alpha^2}\left(2\beta^2+ky\right)^{1/2}\right]^{-1/2}(f^{iv}).
\end{aligned} \tag{53}$$

Collecting coefficients of $\sin\tilde{\alpha}(x-t)$ in equation (52) gives

$$\begin{aligned}
&\rho\sqrt{c^3 d}\left\{\tilde{\alpha}f'' - \left[\frac{4\beta^2}{\alpha^2}y + \frac{k}{2\alpha^2}y^2 - \frac{4\beta\sqrt{2}}{3k\alpha^2}\left(2\beta^2+ky\right)^{3/2} + A\right](\tilde{\alpha}f'') + (\tilde{\alpha}f)\frac{k^2}{4\beta^2\alpha^2}y\right\} \\
&\quad = \left(\frac{k^2 y}{4\beta^2\alpha^2}\right)^2 (g'')\frac{3\alpha\beta}{2\sqrt{2}}\left[\frac{4\beta^2}{\alpha^2} + \frac{k}{\alpha^2}y - \frac{2\beta\sqrt{2}}{\alpha^2}\left(2\beta^2+ky\right)^{1/2}\right]^{-5/2} \\
&\quad - \left(\frac{ky}{4\beta^2\alpha^2}\right)(g''')\alpha\beta\sqrt{2}\left[\frac{4\beta^2}{\alpha^2} + \frac{k}{\alpha^2}y - \frac{2\beta\sqrt{2}}{\alpha^2}\left(2\beta^2+ky\right)^{1/2}\right]^{-3/2} \\
&+\alpha^2(g^{iv}) - \left(\frac{k^2}{4\alpha^2\beta^2} - \frac{3k^3}{16\beta^4\alpha^2}y\right)\frac{\alpha\beta}{\sqrt{2}}(g'')\left[\frac{4\beta^2}{\alpha^2} + \frac{k}{\alpha^2}y - \frac{2\beta\sqrt{2}}{\alpha^2}\left(2\beta^2+ky\right)^{1/2}\right]^{-3/2} \\
&\quad + \alpha\beta\sqrt{2}\left[\frac{4\beta^2}{\alpha^2} + \frac{k}{\alpha^2}y - \frac{2\beta\sqrt{2}}{\alpha^2}\left(2\beta^2+ky\right)^{1/2}\right]^{-1/2}(g^{iv}).
\end{aligned} \tag{54}$$

The equations for $f(y)$ and $g(y)$ can be simplified by assuming that the Reynolds number associated with the present model is small, where the associated Reynolds number is given as

$$\mathrm{Re} = \rho\sqrt{c^3 d}. \tag{55}$$

Therefore,

$$\begin{aligned}
f(y) &= f_0(y) + \mathrm{Re}^2 f_2(y) + \text{higher order terms in Re}, \\
g(y) &= \mathrm{Re}\, g_1(y) + \mathrm{Re}^3 g_3(y) + \text{higher order terms in Re}.
\end{aligned} \tag{56}$$

Hence, evaluating equations (53) and (54) with equation (56) and equating equal terms in Reynolds number, the following ordinary differential equations are obtained for $f_0(y)$ and $g_1(y)$, respectively:

$$\begin{aligned}
&\left(\frac{k^2 y}{4\beta^2\alpha^2}\right)^2 (f_0'')\frac{3\alpha\beta}{2\sqrt{2}}\left[\frac{4\beta^2}{\alpha^2} + \frac{k}{\alpha^2}y - \frac{2\beta\sqrt{2}}{\alpha^2}\left(2\beta^2+ky\right)^{1/2}\right]^{-5/2} \\
&- \left(\frac{ky}{4\beta^2\alpha^2}\right)(f_0''')\alpha\beta\sqrt{2}\left[\frac{4\beta^2}{\alpha^2} + \frac{k}{\alpha^2}y - \frac{2\beta\sqrt{2}}{\alpha^2}\left(2\beta^2+ky\right)^{1/2}\right]^{-3/2}
\end{aligned} \tag{57}$$

$$+\alpha^2\left(f_0^{iv}\right)-\left(\frac{k^2}{4\alpha^2\beta^2}-\frac{3k^3}{16\beta^4\alpha^2}y\right)\frac{\alpha\beta}{\sqrt{2}}\left(f_0''\right)\left[\frac{4\beta^2}{\alpha^2}+\frac{k}{\alpha^2}y-\frac{2\beta\sqrt{2}}{\alpha^2}\left(2\beta^2+ky\right)^{1/2}\right]^{-3/2}$$
$$+\alpha\beta\sqrt{2}\left[\frac{4\beta^2}{\alpha^2}+\frac{k}{\alpha^2}y-\frac{2\beta\sqrt{2}}{\alpha^2}\left(2\beta^2+ky\right)^{1/2}\right]^{-1/2}\left(f_0^{iv}\right)=0. \tag{57(cont.)}$$

$$\left\{\tilde{\alpha}f_0''-\left[\frac{4\beta^2}{\alpha^2}y+\frac{k}{2\alpha^2}y^2-\frac{4\beta\sqrt{2}}{3k\alpha^2}\left(2\beta^2+ky\right)^{3/2}+A\right]\left(\tilde{\alpha}f_0''\right)+\left(\tilde{\alpha}f_0\right)\frac{k^2}{4\beta^2\alpha^2}y\right\}$$
$$=\left(\frac{k^2y}{4\beta^2\alpha^2}\right)^2\left(g_1''\right)\frac{3\alpha\beta}{2\sqrt{2}}\left[\frac{4\beta^2}{\alpha^2}+\frac{k}{\alpha^2}y-\frac{2\beta\sqrt{2}}{\alpha^2}\left(2\beta^2+ky\right)^{1/2}\right]^{-5/2}$$
$$-\left(\frac{ky}{4\beta^2\alpha^2}\right)\left(g_1'''\right)\alpha\beta\sqrt{2}\left[\frac{4\beta^2}{\alpha^2}+\frac{k}{\alpha^2}y-\frac{2\beta\sqrt{2}}{\alpha^2}\left(2\beta^2+ky\right)^{1/2}\right]^{-3/2} \tag{58}$$
$$+\alpha^2\left(g_1^{iv}\right)-\left(\frac{k^2}{4\alpha^2\beta^2}-\frac{3k^3}{16\beta^4\alpha^2}y\right)\frac{\alpha\beta}{\sqrt{2}}\left(g_1''\right)\left[\frac{4\beta^2}{\alpha^2}+\frac{k}{\alpha^2}y-\frac{2\beta\sqrt{2}}{\alpha^2}\left(2\beta^2+ky\right)^{1/2}\right]^{-3/2}$$
$$+\alpha\beta\sqrt{2}\left[\frac{4\beta^2}{\alpha^2}+\frac{k}{\alpha^2}y-\frac{2\beta\sqrt{2}}{\alpha^2}\left(2\beta^2+ky\right)^{1/2}\right]^{-1/2}\left(g_1^{iv}\right).$$

From equation (44), the boundary conditions for $f_0(y)$ and $g_1(y)$ are given as

$$f_0(0)=0,\qquad f_0'(0)=0,\qquad f_0(1)=1,\qquad f_0'(1)=-\psi_{0yy},$$
$$g_1(0)=g_1'(0)=g_1(1)=g_1'(1)=0. \tag{59}$$

The analytical solution to equation (57) is found by using the text [29].

Reducing equation (57) to a second-order equation and then integrating twice, the solution is found. Comparing our reduced second-order equation to and using part 28 on page 134 of text [29] with their notations,

$$\alpha=\frac{A}{E},\qquad \beta=\frac{B}{E},\qquad \gamma=-\frac{C}{E},$$

where

$$A=\frac{k^4 3\alpha\beta\left(4\beta^2/\alpha^2\right)^{-5/2}(14/4)}{2\sqrt{2}\left(4\beta^2\alpha^2\right)^2},$$
$$B=\frac{3k^3\alpha\beta\left(4\beta^2/\alpha^2\right)^{-3/2}(10/4)}{16\beta^4\alpha^2 2\sqrt{2}},$$
$$C=\frac{k^2\alpha\beta\left(4\beta^2/\alpha^2\right)^{-3/2}(10/4)}{4\sqrt{2}\beta^2\alpha^2}, \tag{60}$$
$$D=\frac{k\sqrt{2}\alpha\beta\left(4\beta^2/\alpha^2\right)^{-3/2}(10/4)}{4\beta^2\alpha^2},$$
$$E=\alpha^2+\sqrt{2}\alpha\beta\left(\frac{4\beta^2}{\alpha^2}\right)^{-1/2}\frac{6}{4}.$$

Consequently, with $w_0=f_0''$, equation (57) reduces to

$$w_0''-\frac{D}{E}yw_0'+\frac{1}{E}\left\{Ay^2+By-C\right\}w_0=0. \tag{61}$$

Then, following through the analysis, they describe where

$$s = \frac{D}{4E} \pm \frac{1}{2}\sqrt{\frac{D^2}{4E^2} - \frac{A}{E}} \tag{62}$$

is the root of the quadratic (see [29, p. 134])

$$4s^2 + 2as + \alpha = 0, \qquad a = -\frac{D}{E}, \qquad b = 0. \tag{63}$$

It is found that if we consider the first two terms of the series,

$$\begin{aligned} &w_0 = f_0'' = \exp(hy)\exp\left(sy^2\right) z(\xi), \text{ where } z(\xi) \text{ is found in Table 2.2 of [29, p. 143],} \\ &w_0 = \exp(hy)\exp\left(sy^2\right)\left\{C_1\left[1 + \sum_{n=1}^{\infty}\frac{(a)_n}{(b)_n}\frac{\left(k'\zeta^2\right)^n}{n!}\right]\right. \\ &\left. + C_2 y^{1/2}\left[1 + \sum_{n=1}^{\infty}\frac{(a+1/2)_n}{(b)_n}\frac{\left(k'\zeta^2\right)^n}{n!}\right]\right\}, \end{aligned} \tag{64}$$

where

$$z(\zeta) = \xi\left(a, \frac{1}{2}, k'\zeta^2\right), \qquad \zeta = \frac{y-\mu}{\lambda}, \qquad \mu = -\frac{2b_2h + b_1}{a_1}, \qquad \lambda = 1, \tag{65}$$

$\xi(a, 1/2, k'\zeta^2)$ is the degenerate hypergeometric solution and is found in [29, Part 103, p. 143, Part 65, p. 137].

Subsequently, the solution to equation (57) and hence equations (64) and (65), after applying symbolic integration twice using MATLAB v5.3, is very intricate and given in Appendix A. Numerical solutions of equations (57) for $f_0(y)$ and (58) for $g_1(y)$ result in the plot in Figures 4–7. Figure 3 shows a comparison of $f_0(y)$ with other models [21]. Figure 4 shows the curves for $f_0(y)$ and $f_0'(y)$ with varying values of yield stress. That is, β is gradually varied between zero and unity. Figures 5–7 show curves for $g_1(y)$ and $g_1'(y)$ with varying values of yield stress and various values of wave number. Figure 8 gives a plot of the function, ψ vs. $\bar{x}$, where $\bar{x} = x - t$ as derived in this paper from equations (13),(30)–(32),(45), and (56), which are very similar to plots given in [21].

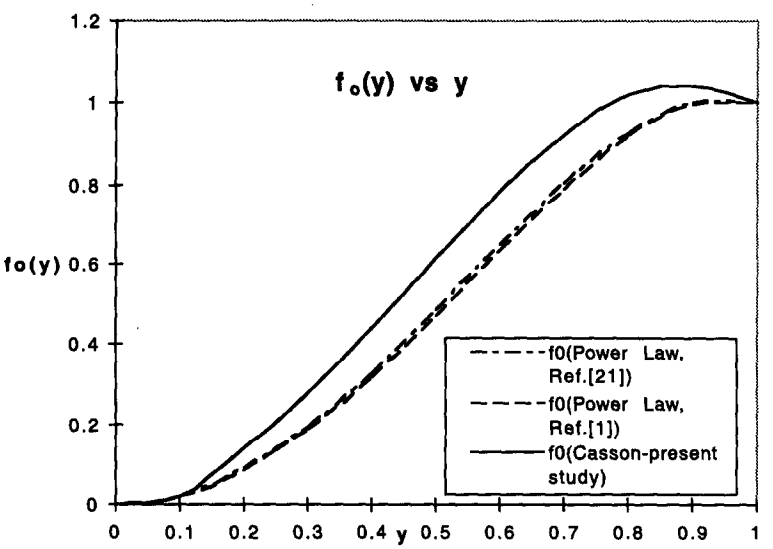

Figure 3. Comparing f_0 vs. y with [21].

When comparing the values of our Casson model in Figure 3, obtained from numerical integration, of the first order in stream function with those of the power-law model of Mernone and Mazumdar [1] and Raju and Devanathan [21], the results are similar but noticeably different. The Casson model indicates the effects of the yield stress and Casson viscosity on the stream function. However, there are similarities between the two models in form. Initially, the two models coincide then diversify as values increase.

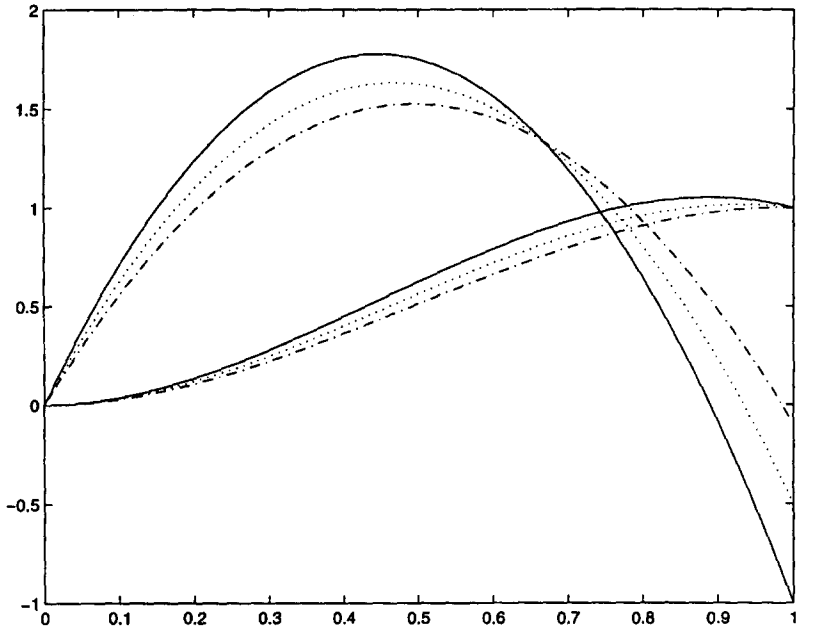

Figure 4. $f_0(y)$ and $f_0'(y)$ with — = $f_0'(1) = -1(\beta = 0), \ldots, f_0'(1) = -0.5$; $-\cdot-\cdot-$ = $f_0'(1) = -0.1(\beta = 1)$.

When considering the $f_0(y)$ and $f_0'(y)$ in Figure 4, it is found that as the yield stress β is gradually varied between zero and unity, the effects on both $f_0(y)$ and $f_0'(y)$ are noticeable and significant. It appears that the maximum value for $f_0'(y)$ is shifted slightly to the right.

Similarly, in Figures 5–7 when considering the functions $g_1(y)$ and $g_1'(y)$, we find that the wave number $\tilde{\alpha}$ has considerable effect on the curves. It appears that as the yield stress β is gradually varied between zero and unity, and therefore the value of $f_0'(y) = -\psi_{0yy}(y)$, there is a shift in the size and shape of the left side and right side in the curve representing $g_1'(y)$. There seems to be a reversal in the location of peaks between the right side and left side. It is of interest to note that the points of inflection occur in exactly the same location when considering each of the respective graphs of $g_1(y)$ and $g_1'(y)$. As the yield stress β is gradually varied between zero and unity, the points of inflection are shifted slightly to the right. The numerical values obtained for $f_0(y)$ and $f_0'(y)$, and $g_1(y)$ and $g_1'(y)$ are indicative of the validity of the perturbation analysis used throughout this research as indicated in equation (45). It is seen that the order in magnitude of $f_0(y)$ is very much greater than that of $g_1(y)$ as is suggested by the perturbation method. From the numerical calculations, we find that the change in behaviour of the streamfunction occurs depending on many parameters, including K, $\tilde{\alpha}$, α, β, R_e, and ε. Just for the sake of understanding peristaltics, we have taken some basic values of the parameters, with $\varepsilon = 0.01$.

When we consider Figure 8, which is a plot of the function ψ given by equations (13) and (30) and equations (45) and (54) and selecting $\varepsilon = 0.01$, for the case of high pressure gradient, with — representing $\psi_{0.1}$ ($y = 0.1$), - - - representing $\psi_{0.3}$, $\cdots$ representing $\psi_{0.5}$, $-\cdot-\cdot-$ representing $\psi_{0.7}$, and $-\cdots-\cdots-$ representing $\psi_{0.9}$ ($y = 0.9$), it is found that the curves for streamfunction ψ run parallel to the axis of the channel when considered near the axis ($y = 0.1$), whereas considerable deformation is observed when they are considered near the boundary ($y = 0.9$). Perhaps a

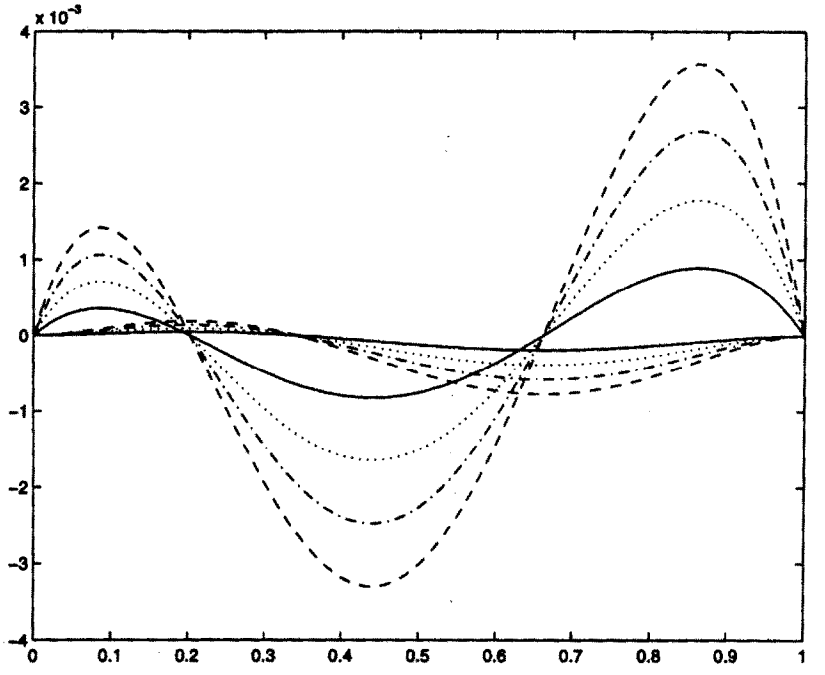

Figure 5. $g_1(y)$ and $g_1'(y)$ with $f_0'(1) = -1$. — = $\tilde{\alpha} = 0.2, \ldots, \tilde{\alpha} = 0.4$; - · - · - = $\tilde{\alpha} = 0.6$; - - - = $\tilde{\alpha} = 0.8$.

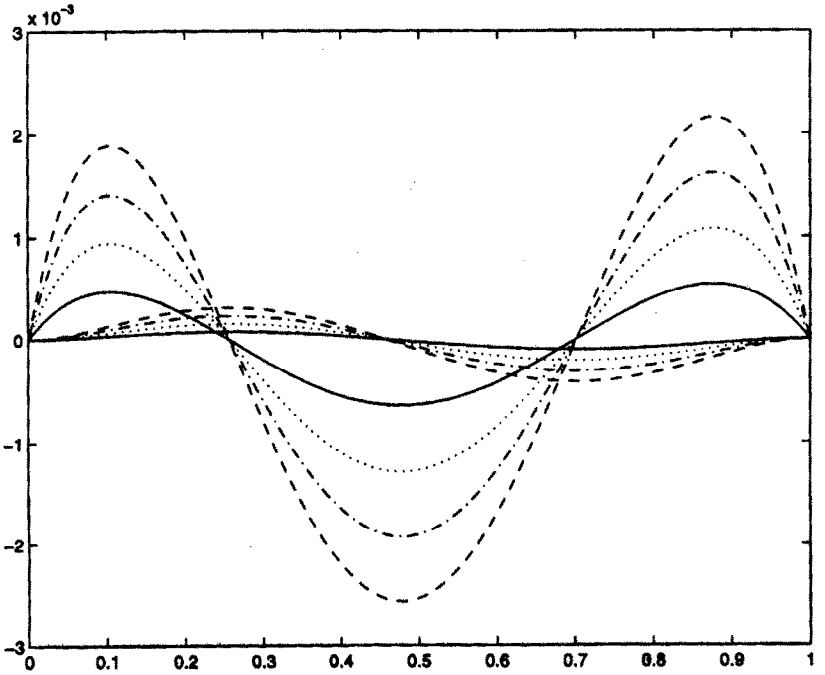

Figure 6. $g_1(y)$ and $g_1'(y)$ with $f_0'(1) = -0.5$. — = $\tilde{\alpha} = 0.2, \ldots, \tilde{\alpha} = 0.4$; - · - · - = $\tilde{\alpha} = 0.6$; - - - = $\tilde{\alpha} = 0.8$.

possible explanation for this sort of behaviour of the streamlines can be given considering the region as consisting of two parts—a central core and a boundary layer region. As the pressure gradient increases, we find that the streamfunctions ψ in the central region are more influenced by it than by the motion of the boundary, and hence the values for the streamfunction run parallel

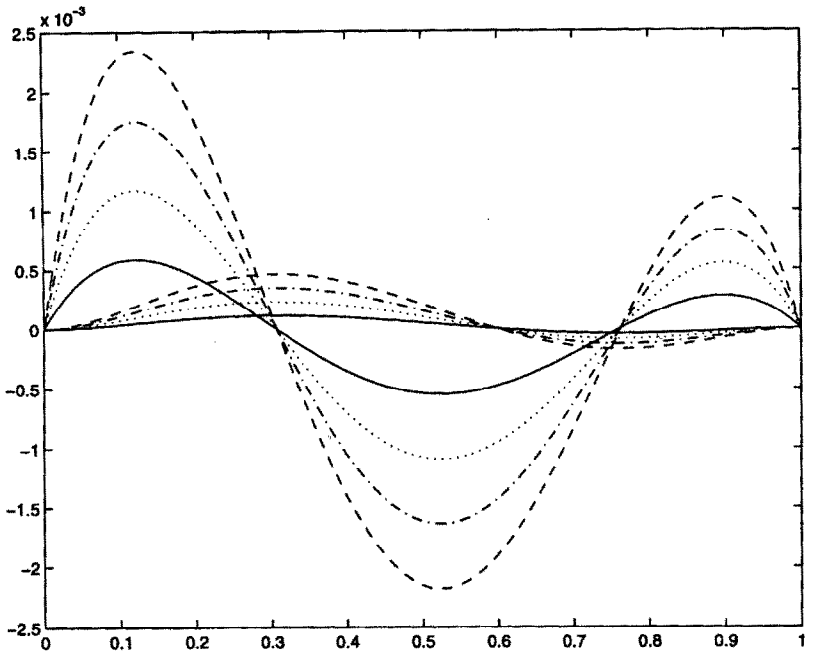

Figure 7. $g_1(y)$ and $g_1'(y)$ with $f_0'(1) = -0.1$. — $= \tilde{\alpha} = 0.2, \ldots, \tilde{\alpha} = 0.4$; – · – · – $= \tilde{\alpha} = 0.6$; – – – $= \tilde{\alpha} = 0.8$.

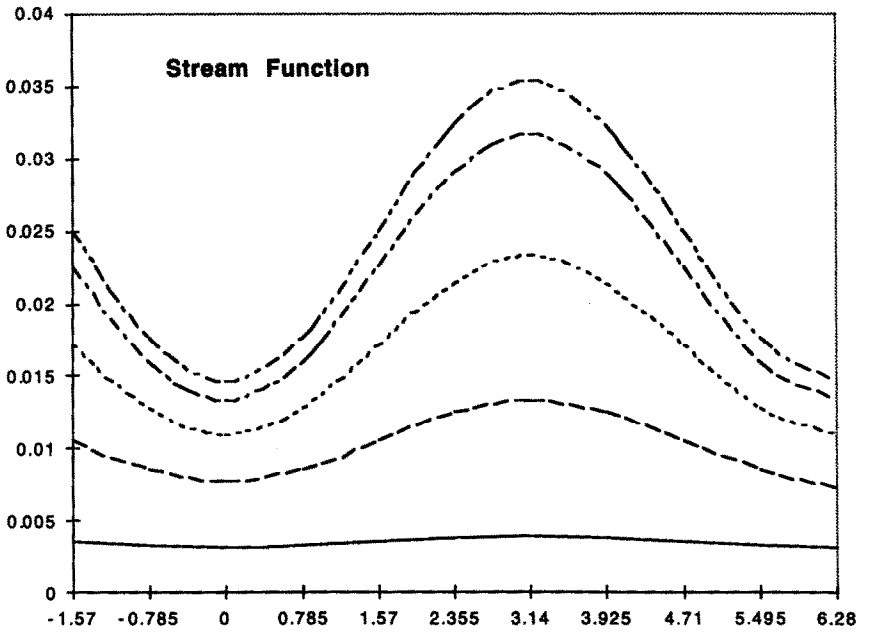

Figure 8. Plot of function ψ vs. $\bar{x}$ as given by equations (30)–(32),(45), and (56).

to the axis, while in the region near the boundary the flow is influenced by both the wave and the pressure gradient.

3. CONCLUSION

In this research it is found that for the Casson model, the governing partial differential equations are indeed extensive and complicated. If, however, we use the fact that zeroth-order perturbation in stream function is a function of the axial coordinate only, because the zeroth-order axial

pressure gradient is constant, we find that the Casson model may be quantitatively expressed as a Newtonian model (Figure 2).

It is found that in the zeroth-order approximation in stream function that there is a dependence on the Casson coefficient of viscosity, yield stress, the density of the fluid, the wave speed, and the dimensions of the channel.

When considering this approximation in the zeroth-order stream function, results show the difference between Newtonian (dashed line) and non-Newtonian (bold line) in Figure 2 seems to be slightly significant, and consistent with that of a Newtonian model, with slight anomalies at very low and very high flow rates.

However, we see that for the first order in stream function the differential equation to be solved is complex, and the analytical solution derived from symbolic integration is more so. The values for the first order in streamfunction are indicative of the perturbation method used, and results in Figures 4–7 are consistent with that given in the literature.

This modelling is appropriate as it may allow insight into the validity of the reduction of the complexity of modelling some non-Newtonian fluids like flow of urine in the ureter and blood flow in the blood vessels under certain physiological conditions.

APPENDIX A

$$f_0 = \frac{C_1\left(1 - 2B^2Ea_1/\Omega b_1\right)}{2}\sqrt{\pi}\exp\left(\frac{h^2}{4s}\right)\frac{1}{s}$$

$$\times\left(\left(s^{1/2}y - \frac{h}{2\sqrt{s}}\right)\operatorname{erf}\left(s^{1/2}y - \frac{h}{2\sqrt{s}}\right) + \frac{\exp\left(-\left(s^{1/2}y - h/2s^{1/2}\right)^2\right)}{\sqrt{\pi}}\right)$$

$$-\frac{C_1}{2}\frac{a_1\Omega^3}{2Eb_1 s}\left\{\begin{array}{l} -\dfrac{\left(-\dfrac{\exp\left(-sy^2+hy\right)}{2s} + \dfrac{h\sqrt{\pi}\exp\left(h^2/4s\right)\operatorname{erf}(\%1)}{4s^{3/2}}\right)}{2s} \\ \quad + \dfrac{1}{2hs}\left(-\dfrac{\sqrt{\pi}\exp\left(h^2/4s\right)\operatorname{erf}(\%1)}{4s^{3/2}}\right. \\ \left. + \dfrac{h\sqrt{\pi}\exp\left(h^2/4s\right)\left(\%1.\operatorname{erf}(\%1) + \exp\left(\%1^2\right)/\sqrt{\pi}\right)}{4s^2}\right) \\ \quad + \dfrac{\sqrt{\pi}\exp\left(h^2/4s\right)\left(\%1.\operatorname{erf}(\%1) + \exp\left(\%1^2\right)/\sqrt{\pi}\right)}{4s^2} \end{array}\right\}$$

$$+\frac{C_1a_1B\sqrt{\pi}}{b_1}\exp\left(\frac{h^2}{4s}\right)\frac{1}{s^{3/2}}$$

$$\times\left(\frac{\operatorname{erf}(\%1)\%1^2}{2} + \frac{\operatorname{erf}(\%1)h\%1}{2s^{1/2}} - 2\frac{-\dfrac{\%1}{4\exp\left(\%1^2\right)} + \dfrac{\sqrt{\pi}\operatorname{erf}(\%1)}{8} - \dfrac{h}{4\sqrt{s}\exp\left(\%1^2\right)}}{\sqrt{\pi}}\right)$$

$$-\frac{C_1a_1B\sqrt{\pi}}{b_1}\exp\left(\frac{h^2}{4s}\right)\frac{1}{s^{3/2}}\left(\frac{\operatorname{erf}(\%1)\%1^2}{2} - \frac{-\dfrac{\%1}{2\exp\left(\%1^2\right)} + \dfrac{\sqrt{\pi}\operatorname{erf}(\%)}{4}}{\sqrt{\pi}} + \frac{\operatorname{erf}(\%1)}{2\sqrt{s}}\right)$$

$$+C_2\left(1 - \frac{2B^2E(a+1/2)}{\Omega b_1}\right)$$

$$\times \sum_{k_2=0}^{\infty} \left(\begin{array}{l} \frac{1}{3} \exp\left(\frac{h^2}{4s}\right) (-1)^{k_2} 2^{(-1-2k_2)} \left(-\frac{h}{\sqrt{s}}\right)^{(-1+2k_2)} y^{3/2} \frac{{}_2F_1\left([3/2, -1-2k_2], [5/2], 2ys/h\right)}{(\sqrt{s}(1/2+k_2)\Gamma(1+k_2))} \\ + \frac{1}{3} 2^{(-1-2k_2)} \exp\left(\frac{h^2}{4s}\right) h(-1)^{k_2} \left(-\frac{h}{\sqrt{s}}\right)^{(2k_2)} y^{3/2} \frac{{}_2F_1\left([1/2, -1-2k_2], [5/2], 2ys/h\right)}{(s(1/2+k_2)\Gamma(1+k_2))} \end{array} \right)$$

$$+ C_2 \left(\frac{\Omega^3 (a+1/2)}{2Eb_1} \right)$$

$$\times \sum_{k_2=0}^{\infty} \left(\begin{array}{l} \frac{1}{7} \exp\left(\frac{h^2}{4s}\right) (-1)^{k_2} 2^{(-1-2k_2)} \left(-\frac{h}{\sqrt{s}}\right)^{(-1+2k_2)} y^{7/2} \frac{{}_2F_1\left([7/2, -1-2k_2], [9/2], 2ys/h\right)}{(\sqrt{s}(1/2+k_2)\Gamma(1+k_2))} \\ + \frac{1}{7} 2^{(-1-2k_2)} \exp\left(\frac{h^2}{4s}\right) h(-1)^{k_2} \left(-\frac{h}{\sqrt{s}}\right)^{(2k_2)} y^{7/2} \frac{{}_2F_1\left([5/2, -1-2k_2], [9/2], 2ys/h\right)}{(s(1/2+k_2)\Gamma(1+k_2))} \end{array} \right)$$

$$+ C_2 \left(\frac{2B (a+1/2)}{b_1} \right)$$

$$\times \sum_{k_2=0}^{\infty} \left(\begin{array}{l} \frac{1}{5} \exp\left(\frac{h^2}{4s}\right) (-1)^{k_2} 2^{(-1-2k_2)} \left(-\frac{h}{\sqrt{s}}\right)^{(-1+2k_2)} y^{5/2} \frac{{}_2F_1\left([5/2, -1-2k_2], [7/2], 2ys/h\right)}{(\sqrt{s}(1/2+k_2)\Gamma(1+k_2))} \\ + \frac{1}{5} 2^{(-1-2k_2)} \exp\left(\frac{h^2}{4s}\right) h(-1)^{k_2} \left(-\frac{h}{\sqrt{s}}\right)^{(2k_2)} y^{7/2} \frac{{}_2F_1\left([3/2, -1-2k_2], [7/2], 2ys/h\right)}{(s(1/2+k_2)\Gamma(1+k_2))} \end{array} \right)$$

$$+ C_3 + C_4,$$

where C_1, C_2, C_3, C_4 are constants of integration determined by the boundary conditions in equation (66), and $\Omega = D - 4sE$ and $\%1 = y\sqrt{s} - h/2\sqrt{s}$.

REFERENCES

1. A.V. Mernone and J. Mazumdar, Mathematical modelling of peristaltic transport of a non-Newtonian fluid, *J. Australasian Physical and Engineering Sciences in Medicine* **21** (3), 126–140, (1998).
2. T.W. Latham, Fluid motion in a peristaltic pump, M.S. Thesis, Massachusetts Institute of Technology, Cambridge, MA, (1966).
3. F. Kiil, *The Function of the Ureter and the Renal Pelvis*, Saunders, Philadelphia, (1957).
4. S. Boyarsky, Surgical physiology of the renal pelvis, *Monogr. Surg. Sci.* **1**, 173–213, (1964).
5. A.H. Shapiro, Pumping and retrograde diffusion in peristaltic waves, In *Proc. Workshop Ureteral Reflux Children*, Nat. Acad. Sci., Washington, DC, (1967).
6. Y.C. Fung and C.S. Yih, Peristaltic transport, *J. Appl. Mech.* **35**, 669–675, (1968).
7. A.H. Shapiro, M.Y. Jaffrin and S.L. Weinberg, Peristaltic pumping with long wavelengths at low Reynolds number, *J. Fluid Mech.* **37**, 799–825, (1969).
8. P.S. Lykoudis, Peristaltic pumping: A bioengineering model, In *Proc. Workshop Hydrodynam. Upper Urinary Tract*, Nat. Acad. Sci., Washington, DC, (1971).
9. S.L. Weinberg, M.Y. Jaffrin and A.H. Shapiro, A hydrodynamical model of ureteral function, In *Proc. Workshop Hydrodynam. Upper Urinary Tract*, Nat. Acad. Sci., Washington, DC, (1971).
10. Y.C. Fung, Peristaltic pumping: A bioengineering model, In *Proc. Workshop Hydrodynam. Upper Urinary Tract*, Nat. Acad. Sci., Washington, DC, (1971).
11. J.C. Burns and T. Parkes, Peristaltic motion, *J. Fluid Mech.* **29**, 731–743, (1968).
12. M. Hanin, The flow through a channel due to traversely oscillating walls, *Israel J. Technol.* **6**, 67–71, (1968).
13. C. Barton and S. Raynor, Peristaltic flow in tubes, *Bull. Math. Biophys.* **30**, 663–680, (1968).
14. N. Liron, A new look at peristalsis and its functions, *Horizons Biochem. Biophys.* **5**, 161–182, (1978).
15. M.G. Mank, Berechnung der peristaltischen Flüssigkeits Forderung mit Method der finiten Element, Dissertation, Hannover, (1976).
16. A.H. Shapiro and T.W. Latham, On peristaltic pumping (abstract), In *Proc. of Annual Conference on Engineering in Medicine and Biology*, Vol. 8, p. 147, Holden Day, San Francisco, (1966).
17. E.C. Eckstein, Experimental and theoretical pressure studies of peristaltic pumping, S.M. Thesis, Dept. Mech. Eng., Massachusetts Institute of Technology, Cambridge, MA, (1970).
18. S.L. Weinberg, Theoretical and experimental treatment of peristaltic pumping and its relation to ureteral function, Ph.D. Thesis, Massachusetts Institute of Technology, Cambridge, MA, (1970).
19. Y.C. Fung and F.C.P. Yin, Comparison of theory and experiment in peristaltic transport, *J. Fluid Mech.* **47**, 93–112, (1971).
20. T.K. Hung and T.D. Brown, Solid-particle motion in two-dimensional peristaltic flows, *J. Fluid Mech.* **73**, 77–96, (1976).
21. K.K. Raju and R. Devanathan, Peristaltic motion of a non-Newtonian fluid, *Rheol. Acta*, 170–179, (1972).

22. L.M. Srivastava and V.P. Srivastava, Peristaltic transport of blood: Casson model II, *J. Biomechanics* **17** (11), 821–829, (1984).
23. L.M. Srivastava, Peristaltic transport of a Casson fluid, *Nig. J. Sci. Res.* **1**, 71–82, (1987).
24. A.M. Siddiqui, A. Provost and W.H. Schwarz, Peristaltic pumping of a second order fluid in a planar channel, *Rheol. Acta* **30**, 249–262, (1991).
25. D. Tang and S. Rankin, Numerical and asymptotic solutions for peristaltic motion of nonlinear viscous flows with elastic boundaries, *SIAM J. Sci. Compt.* **14** (6), 1300–1319, (1993).
26. B. Das and R.L. Batra, Secondary flow of a Casson fluid in a slightly curved tube, *Int. J. Non-Linear Mechanics* **28** (5), 567–577, (1993).
27. J. Elsehawey *et al.*, Peristaltic motion of generalized Newtonian fluid in a non-uniform channel, *J. Phys. Soc. Japan* **67**, 434–440, (1998).
28. Y.C. Fung, *Biomechanics, Mechanical Properties of Living Tissues*, Springer-Verlag, New York, (1981).
29. A.D. Polyanin and V.F. Zaitsev, *Handbook of Exact Solutions for Ordinary Differential Equations*, (1995).
30. Y.C. Fung, *Biomechanics, Motion, Flow, Stress and Growth, Properties of Living Tissue*, Springer-Verlag, New York, (1990).
31. Y.C. Fung, *Biomechanics, Circulation*, Springer-Verlag, New York, (1984).
32. R.L. Batra and B. Jena, Flow of a Casson fluid in a slightly curved tube, *Int. J. Eng. Sci.* **29** (10), 1245–1258, (1991).
33. W.P. Walawender *et al.*, An approximate Casson fluid model for the flow of blood, *Biorheology* **12**, 111–119, (1975).
34. E. Kreyszig, *Advanced Engineering Mathematics*, Fourth edition, Wiley and Sons, (1979).
35. A.M. El Misery, E.F. Elshehawey and A.A. Hakeem, Peristaltic motion of an incompressible generalised Newtonian fluid in a planar channel, *J. Phys. Soc. Japan* **65** (11), 3524–3529, (1996).
36. L.M. Srivastava, V.P. Srivastava and S.N. Sinha, Peristaltic transport of a physiological fluid, Part I, Flow in non-uniform geometry, *Biorheology* **29**, 153–166, (1983).
37. L.M. Srivastava and V.P. Srivastava, Peristaltic transport of a power-law fluid: Application to ductus efferentes of the reproductive tract, *Rheol. Acta* **27**, 428–433, (1988).
38. L. Liethold, *The Calculus with Analytic Geometry*, Third edition, Harper Inter., (1976).